Time-Resolved Fluorescence Microscopy Using an Improved Europium Chelate BHHST for the In Situ Detection of *Cryptosporidium* and *Giardia*

RUSSELL CONNALLY,[1]* DUNCAN VEAL,[1] AND JAMES PIPER[2]
[1]*Department of Biological Sciences, Division of Environmental and Life Sciences, Macquarie University, Sydney, NSW 2109, Australia*
[2]*Department of Physics, Division of Information and Communications Science, Centre for Laser Applications, Macquarie University, Sydney, NSW 2109, Australia*

KEY WORDS time-resolved fluorescence; microscopy; *Cryptosporidium*; *Giardia*; lanthanide chelates; europium; BHHCT; BHHST; immunoconjugate

ABSTRACT Fluorescent immunoconjugates prepared with the europium chelate BHHCT (4,4′-bis(1″,1″,1″,2″,2″,3″,3″-heptafluoro-4″,6″-hexanedion-6″-yl)-chlorosulfo-*o*-terphenyl) have previously been reported as suitable labels for time-resolved fluorescence applications. BHHCT is limited by a tendency to destabilize immunoglobulins when covalently bound to the protein at moderate to high fluorophore to protein ratios (F/P). We report a new derivative of BHHCT prepared by appending a short hydrophylic tether to the chlorosulfonate activating group on BHHCT. The new derivative, BHHST (4,4′-bis-(1″,1″,1″,2″,2″,3″,3″-heptafluoro-4″,6″-hexanedion-6″-yl)sulfonylamino-propyl-ester-*N*-succinimide-ester-*o*-terphenyl), was activated to bind at the tether terminus with a succinimide leaving group that displayed less aggressive coupling activity and improved storage stability. BHHST has been used to prepare a stable and useful immunoconjugate with the anti-*Cryptosporidium* monoclonal antibody CRY104. The BHHST immunoconjugate provides more than a 10-fold enhancement in the signal to noise ratio (SNR) of labeled oocyst fluorescence over background when observed using TRFM techniques. An immunoconjugate was also prepared with BHHST and (goat) anti-mouse that effectively labeled *Giardia* cysts in situ. Detection of cysts with the TRFM was achieved with an 11-fold increase in SNR when a gate-delay of 60 μs was employed. The storage half-life of both immunoconjugates is extended more than 20-fold when compared to immunoconjugates prepared with BHHCT. *Microsc. Res. Tech. 64:312–322, 2004.*

INTRODUCTION

Immunofluorescence microscopy techniques are widely employed, for example, in the specific detection of microorganisms and to identify regions of interest in histophathology samples. There are, however, many instances where the effectiveness of this technique is severely compromised by intrinsic fluorescence (autofluorescence) of the surrounding matrix. The detection of the waterborne pathogens *Giardia lamblia* and *Cryptosporidium parvum* in environmental water bodies requires the concentration of large volumes of water due to the low dose required for infection. The highly concentrated (10,000-fold) water sample is often rich in strongly autofluorescent algae, organic debris, and mineral particles that can obscure immunofluorescently labeled (oo)cysts during analysis. Strong autofluorescence of formaldehyde-fixed tissue samples has also been reported to be commonly encountered and has proven difficult to circumvent (Baschong et al., 2001; Clancy and Cauller, 1998; Sorensen et al., 1997). Both chemical (reduction of the Schiff-bonds) and spectral selection techniques have been employed to reduce fixation-induced autofluorescence (Staughton et al., 2001; Tagliaferro et al., 1997). Spectral selection techniques rely on exciting fluorescence from the target fluorophore with a narrow band of wavelengths that invoke minimal competing fluorescence from the background substrate. Secondly, where possible, the fluorescence emission from the target is spectrally selected to lie outside the pass band of the autofluorescence emission to facilitate exclusion of the latter using narrow passband optical filters. Time-resolved fluorescence techniques exploit the fluorescence lifetime (τ) of fluorophores to differentiate target fluorescence from non-specific background autofluorescence. The majority of natural and synthetic fluorophores have lifetimes measured in nanoseconds; however, certain lanthanide chelates, particularly those of europium and terbium, have τ measured in (several) hundreds of microseconds (Latva et al., 1997; Li and Selvin, 1995; Yuan and Matsumoto, 1998; Yuan et al., 2001). The large difference in τ offered by lanthanide chelates over autofluorophores permits the use of a relatively simple and inexpensive method to enhance the signal-to-noise ratio (S/N) of labelled target. Time-resolved fluorescence techniques exploit the large difference in τ by briefly exciting fluorescence from the sample using a pulsed excitation source. Capture of the resulting fluorescence

*Correspondence to: Russell Connally, Department of Biological Sciences, Division of Environmental and Life Sciences, Macquarie University, Sydney, NSW 2109, Australia. E-mail: rconnall@ics.mq.edu.au

Received 25 May 2004; accepted in revised form 3 August 2004
DOI 10.1002/jemt.20087
Published online in Wiley InterScience (www.interscience.wiley.com).

emission is delayed until the more rapidly decaying autofluorescence has faded beyond detection, whereon the much stronger and slower fading emission from labelled target is collected, typically using an electronically gated image intensified camera (Connally et al., 2002; Hennink et al., 1996; Vereb et al., 1998).

Fluorescence intensity and τ of the chelate is strongly dependent on the chemical nature of the antenna molecule used to capture and transduce energy to the chelated lanthanide cation. The presence of water molecules within the coordination sphere of the lanthanide ion leads to radiationless deactivation of the excited ion and thus the degree to which the antenna molecule shields the ion from water access has a large influence on intensity and fluorescence lifetime. BHHCT is a tetradentate β-diketone chelate that has been demonstrated to be an excellent antenna molecule for the excitation of trivalent europium cations. The molecule has two electron-withdrawing heptafluoro groups that flank the β-diketone moiety and help promote enol formation to strongly bind the lanthanide ion. The heptafluoro groups also impart increased hydrophobic character to the fluorophore that ultimately restricts the number of molecules that may be bound to immunoglobulin.

Consideration must also be given to the effects on protein folding that can arise from the close proximity of the relatively large BHHCT molecule in immunoconjugates. BHHCT is activated to bind with protein by treatment with chlorosulfonic acid to form the chlorosulfonate and subsequent reaction with protein results in close attachment of BHHCT to the protein via a single sulfur atom. The high activity of the chlorosulfonate permits bonding with primary and secondary amines as well as amino-acid residues containing hydroxy groups. A further problem with BHHCT arises from the difficulty in preparing the pure compound. Preparation of BHHCT, even from pure BHHT, resulted in a product mixture when examined using reverse phase thin-layer chromatography (TLC). A portion of these mixed products appear to actively bind to protein but have little or no fluorescence yield, thus diluting the effective F/P ratio. At low F/P ratios, fluorescence intensity of target labeled with the immunoconjugate is largely dependent on the number of bound BHHCT molecules. However, at high F/P ratios antibody activity was rapidly degraded and inactive preparations often resulted. Different immunoglobulins were observed to display different sensitivities to inactivation. A useful BHHCT immunoconjugate against *Giardia lamblia* was readily prepared whereas anti-*Cryptosporidium* (CRY104) immunoconjugates were consistently inactive. To overcome these limitations, a 5-atom hydrophylic molecular tether was attached to BHHCT via the chlorosulfonate and the BHHCT derivative was then activated to bind to proteins as the succinimide. The new compound could be prepared in high purity by simple chemical methods and was far more stable than the chlorosulfonate on storage. Addition of a BHHST solution to protein solution results in a release of succinimide that can be monitored spectrophotometrically to follow the course of the conjugation.

MATERIALS AND METHODS

Instrumentation

The time-resolved fluorescence microscope (TRFM) used in the present study has been described in detail previously (Connally et al., 2002). In brief, the TRFM was built using a conventional epifluorescence microscope equipped with a pulsed excitation source (flashlamp) and a time-gated image-intensified CCD camera. The whole is controlled by a microprocessor to synchronize the excitation and capture sequence. The microscope was fitted with a UV excitation filter and a longpass emission filter set typically employed for the examination of DAPI (4′,6-diamindino-2-phenylindole) stained samples.

Fluorescence lifetime of the chelates BHHST and BHHCT was measured on a FluoroStar Galaxy spectrophotometer (BMG Lab Technologies, GmbH, Offenburg, Germany).

Reagents

Conjugation buffer: sodium bicarbonate ($NaHCO_3$; 0.1 M, pH 9.0) pH adjusted with 1N sodium hydroxide. Fresh reagent was prepared for each conjugation. Phosphate buffered saline (PBS, pH 7.4; 150 mM NaCl, 15 mM KH_2PO_4, 20 mM Na_2HPO_4, 27 mM KCl) 1 × Aldrich P-4417 tablets in de-ionized water (200 ml). Fluorescence enhancing buffer (FEB) was prepared by adding Triton X-100 at 3 $mg.ml^{-1}$, trioctylphosphine oxide (TOPO) at 0.6 $mg.ml^{-1}$ and Tween 80 at 2.6 $mg.ml^{-1}$ to 0.1 M bicarbonate buffer at pH 8.5. Europium chloride stock solution was prepared by dissolving 100 mg of europium oxide (Eu_2O_3) in 3 ml of concentrated hydrochloric acid and evaporating to dryness under vacuum (water-pump) on a boiling water bath. The solution was re-dissolved in deionized water (1 ml) and again evaporated to dryness under vacuum on the water bath to remove traces of HCl. The salt was then dissolved in deionized water and transferred to a 25-ml volumetric flask to give a 22.7 mM solution. Methanolic europium chloride solution for spraying on TLC plates was prepared by diluting an aliquot of the stock solution to 2-mM concentration with deionized water and mixing with an equal volume of methanol containing 20 μM Triton X-100. Polyvinyl alcohol thickened europium chloride solution (PVA-Eu^{3+}) was employed to reduce evaporation and retard the movement of (oo)cysts during microscopy. Polyvinyl alcohol (mw 30,000–70,000; 40 $mg.ml^{-1}$) was dissolved in europium chloride solution (7.5 mM). The 10,000:1 concentrate of environmentally sourced water used for this work was a kind gift from Dr. Belinda Ferrari and was prepared from 10-L backwash water samples using the flocculation method (Vesey et al., 1993).

Measurement of Chelate Fluorescence Lifetime (τ)

An aliquot of BHHCT (~320 μg) was dissolved in 1,4 dioxane (100 μL) and the solution further diluted (3 μL in 97 μL 1, 4 dioxane) to give a 0.12 mM stock solution. An aliquot of BHHST (~400 μg) was similarly treated to give a 0.122 mM stock solution. Duplicate wells were prepared with fluorescence enhancing buffer (100 μL), europium chloride solution (220 μM; 2 μL) and 1 to 3 μL of each chelate stock solution. Time-resolved fluorescence intensity measurements were taken after an

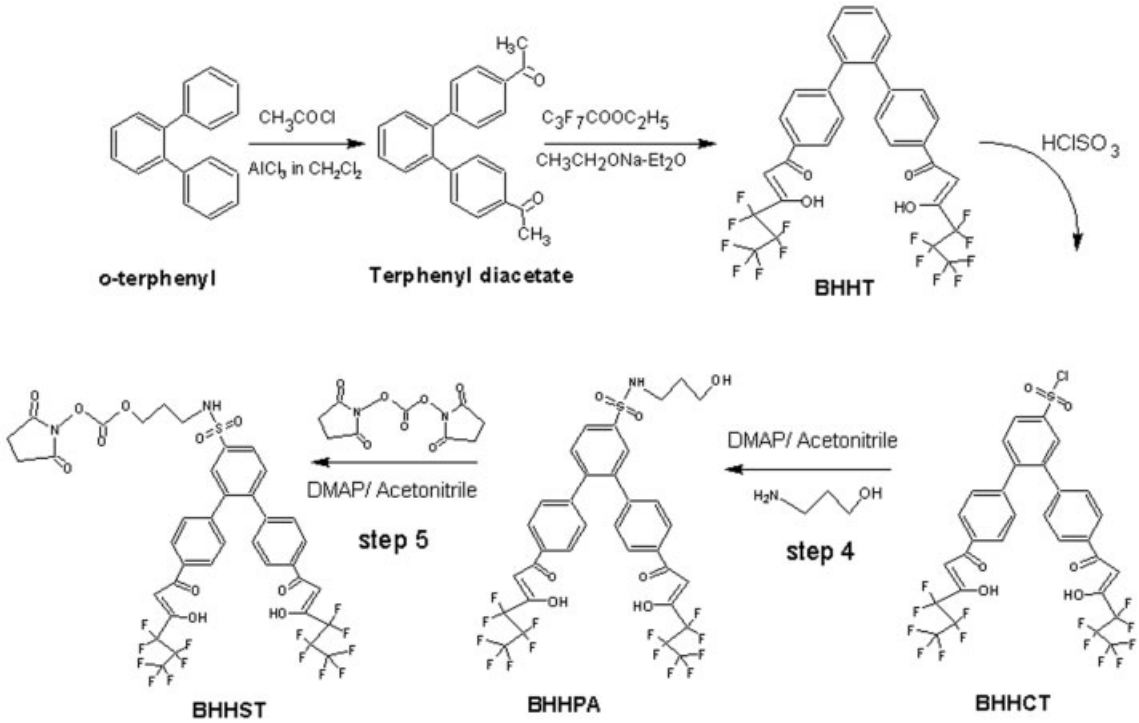

Fig. 1. Synthetic scheme used to produce BHHST relied on the use of DMAP in acetonitrile to facilitate the reaction.

initial delay of 100 μs with increments of 100 μs. The $\log_n$ of fluorescence intensity was plotted against time to give a line with slope equal to the negative reciprocal of the fluorescence lifetime in microseconds.

Fluorescent Chelate Synthesis

BHHCT was prepared by a method previously reported (Yuan and Matsumoto, 1998) using the scheme shown in Figure 1 that also outlines the method employed to produce BHHST.

BHHPA (4,4′-bis(1″,1″,1″,2″,2″,3″,3″-heptafluoro-4″,6″-hexanedion-6″-yl)-(3-hydroxy-propyl)- sulfonamide)-*o*-terphenyl) was prepared as follows: BHHCT (1.21 g; 142 mM) in dry acetonitrile (25 ml) was transferred to a 100-ml round bottom flask containing a magnetic stirrer bar. To this was added, alternately in 500-μl aliquots, solutions of dimethylaminopyridine in acetonitrile (4.1 mM; 500 mg in 5 ml), and 3-aminopropanol in acetonitrile (2.9 mM; 220 mg in 5 ml). On addition of the two solutions, the BHHCT solution became momentarily cloudy but rapidly cleared to form an orange-yellow solution that was stirred for a further 3 hours before terminating the reaction. The reaction proceeded rapidly as followed using reverse-phase TLC (3:2 MeOH:H_2O) and was essentially complete after 1 hour. The appearance of by-products occurred simultaneously with the formation of BHHPA and these impurities were removed by acid-wash in the workup. Acetonitrile was removed at 45°C on the rotary evaporator and the residue dissolved in ethyl acetate/$KHSO_4$ (200 ml) solution and transferred to a separatory funnel. Note the organic material is insoluble in the ethyl acetate until acidified. The organic phase was washed (3 × 20 ml) with aqueous $KHSO_4$ (15 g.100 ml^{-1}) followed by (2 × 50 ml) brine washes and then dried over drierite (overnight). Ethyl acetate was removed on the rotary evaporator to give 1 g of crude BHHPA (79% yield) that was refluxed for 2 hours with a liter of water-saturated hexane (1 ml water in 1 L hexane). The hexane solution was filtered and reduced on the rotary evaporator to give 120 mg of purified BHHPA and the process was repeated several times until all the BHHPA had been extracted. BHHPA has low solubility in wet hexane (about 120 μg.ml^{-1}) and very low solubility in dry hexane. However, the impurities are far less soluble in this solvent, wet or dry. ^{1}H NMR δ (400 MHz, $CDCl_3$) 1.80 (2H quintet), 3.25 (2H quartet), 3.81 (2H t), 5.22 (1H, t), 6.58 (2H, s), 7.28 (4H, split doublets), 7.61 (1H, d), 7.86 (4H, split doublets), 7.97 (2H, t), 7.99 (1H, d); Electrospray-MS, m/e 843.

BHHST-(4,4′-bis-(1″,1″,1″,2″,2″,3″,3″-heptafluoro-4″,6″-hexanedion-6″-yl)sulfonylamino-propyl ester *N*-succinimide-ester-*o*-terphenyl) was prepared from the hexane treated BHHPA.

Purified BHHPA (270 mg; 320 μM) was dissolved in acetonitrile (15 ml) in a 50-ml round bottom flask equipped with a stirrer bar. Acetonitrile solutions of di-(*N*-succinimidyl) carbonate (DSC: 600 μM; 165 mg in 1 ml) and dimethylaminopyridine (DMAP: 800 μM; 100 mg in 1 ml) were prepared. The BHHPA solution was purged with argon as the DSC and DMAP solutions were added in alternate aliquots. After addition of the DSC/DMAP, a TLC sample was taken and the flask filled with argon, stoppered and stirred magnetically. A second TLC sample was taken 3 hours later and the contents stirred for a further 45 hours before solvent was removed on the rotary evaporator at 45°C and the

TABLE 1. Volume and concentration of reagents used for conjugation with immunoglobulin

Code	Antibody	Ab. conc.	BHHST vol.	BHHST conc.
O_1	100 μL of CRY104	5.9 mg.ml^{-1}	11 μL	1.42 mg.ml^{-1}
O_3	100 μL of Antimouse	3.3 mg.ml^{-1}	11 μL	1.42 mg.ml^{-1}

residue dissolved in ethyl acetate (200 ml). The organic phase was washed (3 × 20 ml) with aqueous $KHSO_4$ (15 g.100 ml^{-1}) followed by (2 × 50 ml) brine washes and then dried over drierite (overnight). The ethyl acetate was removed on the rotary evaporator to give 200 mg of crude BHHST (63% yield) that was further purified by solution in hexane (approximate solubility 1 mg.ml^{-1}). Four fractions were obtained in each (100 ml) extraction weighing successively 100, 65, 17, and 3 mg; the remaining red-colored hexane-insoluble residue weighed 20 mg. Sample from the 65-mg hexane fraction was reserved for NMR analysis. ^{1}H NMR δ (400 MHz, $CDCl_3$) 2.18 (2H quintet), 3.10 (2H t), 4.04 (2H t), 4.35 (2H t), 6.57 (2H s), 7.29 (4H, t), 7.61 (1H, s), 7.63 (1H, s), 7.86 (4H, t), 8.13 (1H, s), 8.15 (2H, d).

Antibodies: Desalting and Exchange With Conjugation Buffer

The monoclonal anti-*Cryptosporidium* antibody CRY104 (Ausflow, Macquarie Research Limited, NSW, Australia) contained sodium azide that was removed using Millipore Ultrafree-0.5 50K centrifugal filters. The antibody (500 μL.; 3.3 mg.ml^{-1}) was reconstituted with conjugation buffer (pH 9.04) after desalting to give a solution of half the original volume (200 μL). Using Eq. 1, protein concentration was estimated using the absorbance at 280 nm and a conversion constant of 1.38 to convert to concentration in mg.ml^{-1} (5.9 mg.ml^{-1}). Lyophilized anti-mouse polyvalent immunoglobulin was reconstituted using conjugation buffer to give a final protein strength of 3.3 mg.ml^{-1} as shown in Table 1.

$$\text{Desalted antibody concentration (mg.ml}^{-1}) = \frac{A_{280}}{1.38} \quad (1)$$

Preparation of BHHST solution

A 1-mg aliquot of BHHST was dissolved in 80 μL of DMF and a 3-μL sample serially diluted (33:1 then 20:1 in conjugation buffer) to give a final dilution of 667:1.

The concentration of BHHST was determined using the molar absorbance coefficient (ε_{320}) of 3.32 × 10^4 cm^{-1}.M.L^{-1}. Duplicate samples were analyzed and averaged to determine BHHST concentration, estimated to be 14.4 mg.ml^{-1}.

Conjugation of Fluorophore to Protein

CRY104 antibody (100 μl: 5.9 mg.ml^{-1}) and anti-mouse immunoglobulin (100 μl: 3.3 mg.ml^{-1}) were reacted at room temperature for 1 hour with BHHST (11 μl: 14.4 mg.ml^{-1}). The crude immunoconjugates were then filtered (Millipore Ultrafree 0.2 μm) to remove any precipitate and unbound chelate removed using Ultrafree Biomax 50K centrifugal filters. Filters were loaded with conjugation product (110 μL) and diluted with 100 μL of PBS. Centrifugation was performed at 13,000 RPM in a cool room at 4°C for 25 min. or until the residue in the filter was reduced to a volume of 15 μL. A further 100 μL of PBS was added to the filter and volume again reduced to 15 μL whereupon a final wash with another 100 μL of PBS was performed. The immunoconjugates were then taken up in 100 μL of 0.1M of $NaHCO_3$ solution and filtered (Millipore Ultrafree 0.2 μm) to remove any precipitate. Filtrate from each centrifugal wash operation was analyzed on a spectrophotometer to monitor removal of unbound BHHST from the immunoconjugate.

Protein concentration and F/P ratios were determined using Eq. 2 where A_{320} and A_{280} are absorbance readings at 320 and 280 nm, respectively, and ε_{320} is the molar absorbance coefficient of BHHST (3.32 × 10^{4}M.L^{-1} cm^{-1}). The experimentally determined A_{280}/A_{320} ratio of BHHST (δ parameter) was estimated to be 0.60, both goat and mouse antibody have a molecular weight of 150,000. The divisor of 1.38 was used to convert immunoglobulin absorbance readings directly into concentration in mg.ml^{-1} using Eq. 1.

$$\text{F/P ratio} = \left(\frac{A_{320}}{\varepsilon} \times \text{dilution}\right) \times \frac{150{,}000}{\left(\frac{A_{280} - (A_{320} \times \delta)}{1.38} \times \text{dilution}\right)} \quad (2)$$

In Situ Direct Labeling of *Cryptosporidium* Oocysts With Immunoconjugate

Labeling of (oo)cysts was performed 36 days after preparation of the immunoconjugates; For the direct labeling of *Cryptosporidium* oocysts with immunoconjugates O_1, an aliquot of PBS spiked with oocysts (10 μl containing 7.5 × 10^7 oocysts.ml^{-1}; 90 μL PBS) was combined with water concentrate (200 μL) in a micro-reaction vial. An aliquot (100 μL) was then applied to a membrane filter (Millipore Isopore membrane filter, 0.8 μm) followed by washing with conjugation buffer (3 × 100 μL). The filter was then incubated with immunoconjugate O_1 for 30 minutes at 4°C followed by further washing with fluorescence enhancing buffer (FEB; 3 × 100 μL). The filter was then transferred to a micro-reaction vial (kept at 4°C) containing 40 μL of FEB and vortexed to release the labeled cysts and water concentrate debris from the membrane. An aliquot (3 μL) of the labeled water concentrate was combined with an equal volume of the PVA/Eu^{3+} solution on a microscope slide for analysis using the TRFM.

In Situ Indirect Labeling of *Cryptosporidium* Oocysts

Pre-treatment of the spiked water concentrate with native (unlabeled) anti-*Cryptosporidium* immunoglobulin was performed (100 μl; 165 μg.ml^{-1}) following the protocol described above for in situ direct labeling of

TABLE 2. Immunoconjugate F/P ratio

Conjugate	Code	Diln.	A_{280}	A_{320}	Adj. A_{280}	Protein ($\mu g.ml^{-1}$)	Chelate ($\mu g.ml^{-1}$)	F/P ratio	% Yield
CRY104	O_1	33:1	0.149	0.099	0.087	2142	82.8	5.9	36
Antimouse	O_3	33:1	0.067	0.069	0.024	612	63.5	15.8	19

oocysts. The labeled anti-mouse immunoconjugate was then applied to the membrane (100 μl; 66 $\mu g.ml^{-1}$) for an incubation period of 20 minutes at 4°C. The filter was then washed and treated as described for the direct labeled samples.

Comparison of the Relative Water Solubility of BHHCT and BHHST

Previously, immunoconjugates with BHHCT were prepared by adding a 1,4 dioxane solution of the chelate to an aqueous solution of the protein. When 1,4 dioxane solutions of BHHCT exceeded 12 mM in concentration, immediate precipitation of a portion of the chelate occurred on addition to the buffered protein solution whereas higher concentrations of BHHST were required before similar precipitates were observed. The difference in sensitivity to precipitation in aqueous media (0.1 M $NaHCO_3$) was quantified by preparing solutions of both BHHST and BHHCT at similar molar concentrations in 1,4 dioxane and measuring the optical density of the aqueous buffer as chelate was incrementally added. The validity of the test rests on the assumption that optical density is increased by the presence of chelate precipitate that scatters the incident beam ($\lambda = 600$ nm). An Eppendorf Biophotometer 6131 was used to perform the measurement using the OD600 protocol. The chelate solutions were adjusted to approximately 26 mM and added in 1-μL increments to 100 μL of $NaHCO_3$ buffer whilst recording the optical density.

Calculation of the Improvement in Signal to Noise (S/N) Ratio Using TRFM

In time-resolved fluorescence applications, the gate-delay period follows the light excitation pulse and duration of this period is controlled to ensure complete decay of both sample autofluorescence and faint light emission from the decaying flashlamp plasma. The ratio of the cyst fluorescence signal ($Icyst_N$) to that of the autofluorescence or noise signal ($Iauto_N$) was determined at different gate-delay periods. This ratio was in turn divided by the ratio of fluorescence intensities for the autofluorophore ($Iauto_0$) and the cyst ($Icyst_0$), with the microscope operated in conventional epifluorescence mode to calculate Δ(S/N).The enhanced response was determined using Eq. 3 where I_0 and I_N are peak pixel intensities after gate-delays of 0 and N μs, respectively.

$$\Delta(S/N) = \frac{\left(\frac{Icyst_N}{Iauto_N}\right)}{\left(\frac{Iauto_0}{Icyst_0}\right)} \quad (3)$$

RESULTS

Immunoconjugate Properties

The final concentration and the calculated F/P ratio for the immunoconjugates is shown in Table 2 and is based on the analysis of duplicate samples from each preparation. After removal of unbound BHHST, the volume of each immunoconjugate was adjusted to 100 μl with PBS solution and significant protein loss was observed for both immunoconjugates. The mouse immunoconjugate O_1 was obtained in 36% yield whereas the anti-mouse polyvalent immunoglobulin was collected in about 19% yield.

Time-Resolved Fluorescence Microscopy

We have previously reported the efficacy of spectral selection techniques alone, and in conjunction with TRFM, to decrease the intensity of autofluorescent emission (Connally et al., 2004). For this report, however, autofluorescence emission was suppressed solely through the application of a time-resolved fluorescence techniques and the TRFM was fitted with a longpass (DAPI) emission filter.

Photophysics of BHHST and BHHCT

The absorbance spectrum for BHHST and BHHCT are nearly identical (see Fig. 2) although the molar absorbance coefficient (ε_{320}) is higher for BHHST (3.32×10^4) compared to BHHCT (2.8×10^4). Fluorescence spectra are shown in Figure 2 (right) for the chelates complexed with europium and again little difference between the two can be discerned. Both chelates show a strong peak in fluorescence emission at 617 nm when complexed with europium corresponding to the ^5D_o to $^7F_1$ transition for this lanthanide. As reported by Yuan et al. (1998), buffer environment has a strong influence on fluorescence intensity and lifetime (τ) with superior results obtained for chelates suspended in bicarbonate buffer (0.1 M; pH 8.5) containing TOPO. With reference to the plot shown in Figure 3, there was a small difference in τ observed for BHHCT and BHHST in bicarbonate buffer with values of 625 and 602 μs, respectively, averaged over three different concentrations (1 to 3 μM).

Direct Labeling of *Cryptosporidium* Oocysts With Immunoconjugate O_1

A comparatively large number of *Cryptosporidium* oocysts were injected into the water concentrate used for the in situ labeling experiment and, consequently, most autofluorescent components were found associated with several oocysts. The arrangement of the oocysts decorating the spines of the desmid (see Fig. 4) was fortuitous since it conveniently provided a strongly autofluorescent component that helped illustrate the power of TRFM to increase the S/N ratio by suppressing autofluorescence. Fluorescence intensity of the BHHST label was sufficient for TRFM studies even though probe intensity was only marginally greater than the fluorescence signal emitted by the autofluorescent desmid (in conventional epifluorescence mode). A small speck of precipitated immunoconjugate was visible at the terminus of the bottom spine situated just below the central oocyst in Figure 4b. The precipitation

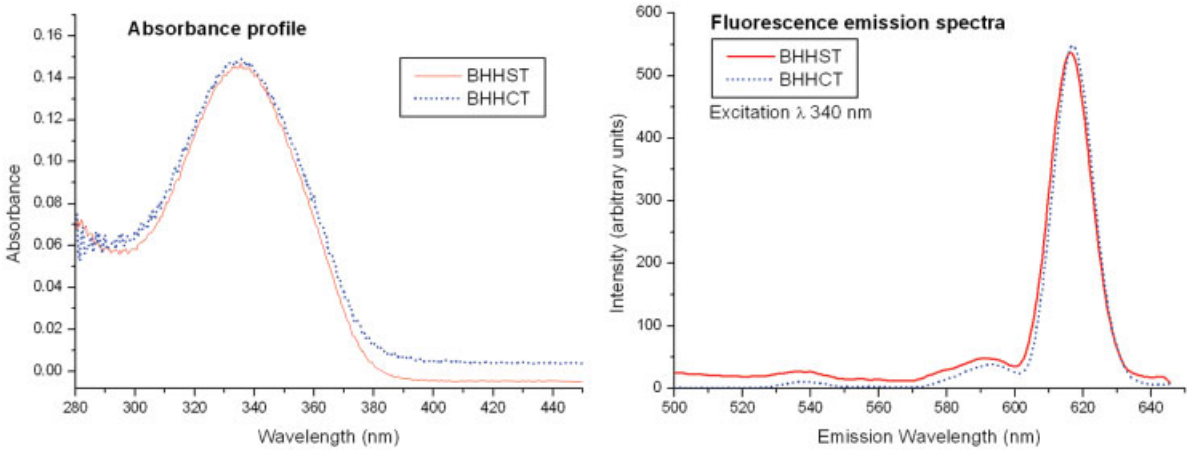

Fig. 2. The absorbance and fluorescence characteristics of BHHST are very similar to those of BHHCT although the molar absorbance coefficient of the former compound was determined to be higher (3.32×10^4 vs. 2.8×10^4). The fluorescence spectra is shown for the chelates complexed with trivalent europium ions. [Color figure can be viewed in the online issue, which is available at www.interscience.wiley.com.]

of immunoconjugate occurred during the incubation phase with the water sample. Precipitation was observed to increase when the pH of the bicarbonate FEB solution was greater than 8.5. Determination of the improvement in S/N for Figure 4 was performed by sampling pixel values across the centre of the desmid in conventional and time-resolved modes to report the magnitude of autofluorescence suppression. This value was in turn compared with the ratio of intensities observed for a BHHST labeled oocyst. The oocyst situated at the bottom right of Figure 4 was selected for measurement since the pixel intensities were within the 8-bit range (255 grey-scales) employed for image capture. The other three oocysts, although brighter, had regions with pixel intensities that reached the upper limit causing a loss of information on the true pixel intensity. The extent of autofluorescence suppression can be more readily appreciated by referring to the line profile shown in Figure 5 (left). This profile is for a line transecting the desmid centre and shows a reduction from an average pixel intensity of 187 to 17 (8-bit range) in time-resolved mode. The labeled oocyst profile (Fig. 5, right), however, was observed to show a modest 20% drop in fluorescence intensity after a gate-delay of 60 μs but autofluorescence was suppressed 11-fold in TRFM mode resulting in an improvement in S/N from 0.8 in conventional epifluorescence mode to 7.1 with TRFM. Using Eq. 1, the effective overall improvement in S/N achieved with TRFM and direct label immunoconjugate was determined to be 8.8 (Table 3).

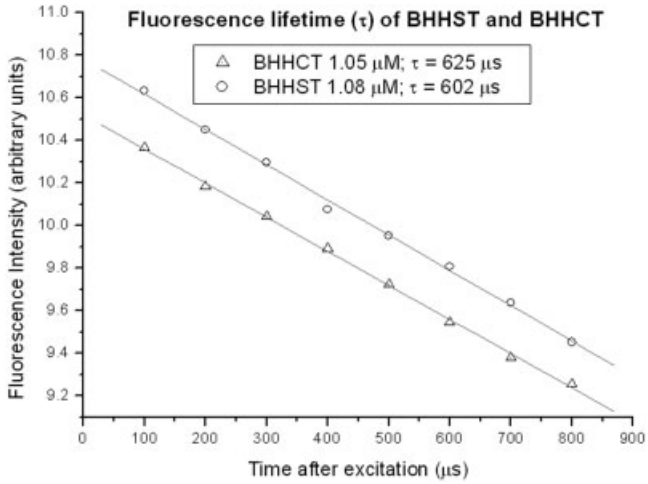

Fig. 3. Fluorescence lifetime for BHHST and BHHCT was measured in bicarbonate buffer containing TOPO using a 1-μM chelate solution complexed with an excess of europium ions. Fluorescence decay for these compounds is known to follow single exponential decay kinetics and τ is equal to the negative reciprocal of the gradient for the line obtained by plotting $\log_n$ intensity over time. BHHST was observed to have marginally shorter τ (602 μs) than that observed for BHHCT (625 μs).

Indirect Labeling of *Giardia* Cysts With Immunoconjugate O_3

The anti-mouse BHHST immunoconjugate was employed using an indirect in situ labeling protocol whereby the water concentrate (spiked with *Giardia lamblia*) was pretreated with a monoclonal antibody against *Giardia* before application of the anti-mouse conjugate. Autofluorescence was suppressed 11.7-fold in TRFM mode to achieve an 11.1-fold increase in S/N ratio for the labeled *Giardia* cyst over background as calculated using Eq. 3. Table 3 summarizes the S/N response for both conjugates analysed with conventional (epifluorescence) mode and reports the effective improvement Δ(S/N) when time-resolved fluorescence mode was employed. Traces of the BHHST anti-mouse immunoconjugate remained with the filtrate (see Fig. 6) resulting in a slight increase in background. The meandering ridge visible to the right of the cyst in TRFM mode delineates an increase in local concentration of the time-resolvable immunoconjugate at the buffer boundary. Although not readily visible in the photomicrograph of Figure 6 (far left), the ridge is visible in the line profile (Fig. 6, right). The line profile also illustrates the fact that fluorescence intensity from

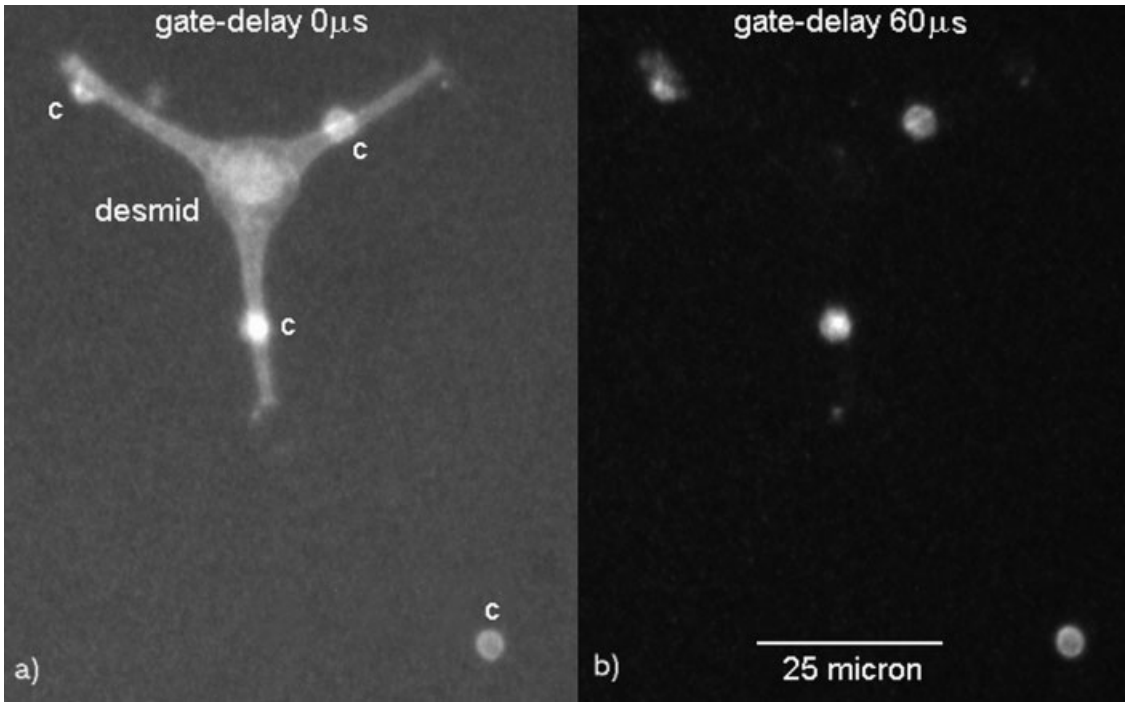

Fig. 4. The trigonal object (**left**) is an autofluorescent desmid (*Chlorophyta staurastrum*) in contact with (3) immunofluorescently labeled oocysts (labeled c). **a:** A gate-delay of 0 μs, image-intensifier gain of 50. **b:** A gate-delay of 60 μs and an image-intensifier gain of 60. Both images acquired with loop-count of 250 and a 10-ms exposure period with 2 × 2 pixel binning.

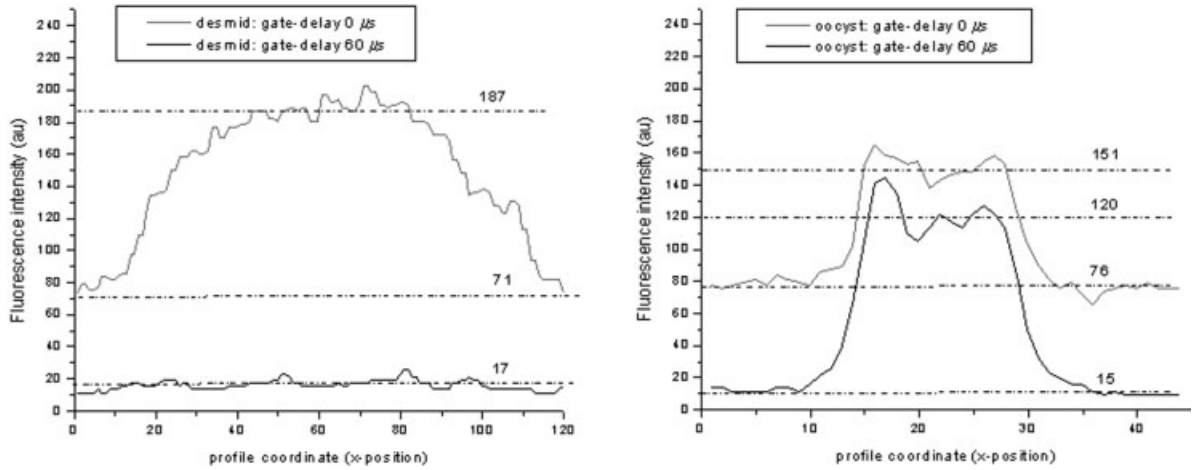

Fig. 5. **Left:** The autofluorescence intensity measured across the centre of the desmid shown in Figure 4 at gate-delays of 0 and 60 μs. **Right:** Corresponds to a line sample that transects the oocyst labeled "c" at the bottom right of Figure 4a, measured at gate-delays of 0 and 60 μs.

the *Giardia* cyst was undiminished in time-resolved mode after a gate-delay of 60 μs with an average value of 158. Background fluorescence levels, however, were significantly reduced from an average pixel value of 77 to 13. The level of autofluorescence suppression was conservatively estimated since regions selected for analysis were at moderate brightness levels only. The autofluorescence suppression and S/N factors are superior when regions of high brightness are selected for analysis. However, pixel information is lost when fluorescence intensity lies at the upper bound of the 12-bit dynamic range of the camera.

Relative Hydrophilicity Comparison Between BHHST and BHHCT

Figure 7 is a plot of the optical density as measured using the OD600 protocol and a significant difference in opacity was observed between aqueous solutions of BHHST and BHHCT of similar concentration. The greatest optical density for BHHST was observed at a

TABLE 3. Effective signal-to-noise ratio (S/N) for the (oo)cysts measured against background was compared using conventional epifluorescence mode and TRFM mode

Sample region		Non-TRFM			TRFM-60μs			
Figure	Region analyzed	Mean	SD	S/N	Mean	SD	S/N	ΔS/N
4	Autofluorescence	187	6.3		17	2.7		
	Crypto. oocyst	151	7.1	0.8	120	12.6	7.1	8.8
6	Autofluorescence	208	13		17.8	1.5		
	Giardia oocyst	166	6.2	0.8	158	15	8.9	11.1

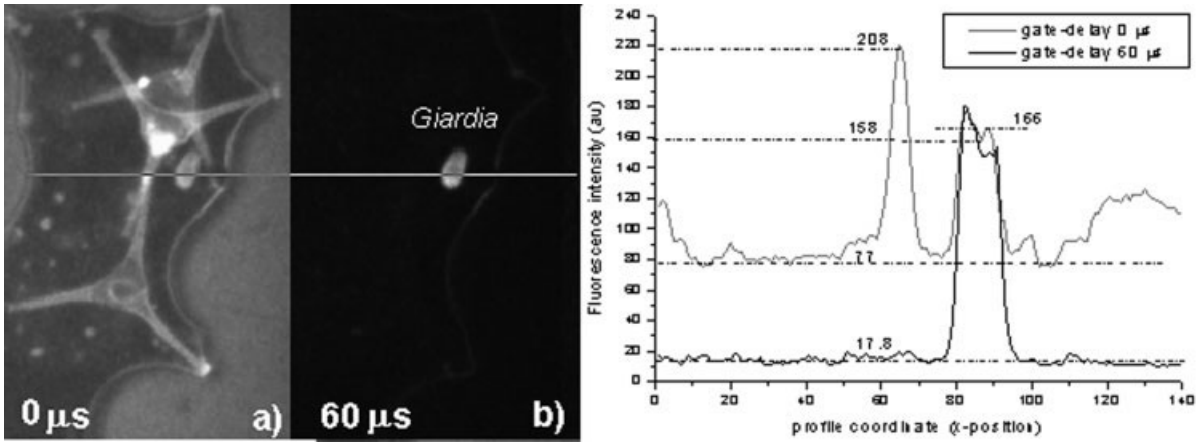

Fig. 6. Left: Anti-mouse immunoconjugate labeled *Giardia lamblia* cyst together with three autofluorescent desmids. Images acquired in conventional epifluorescence mode (**a**) and with a gate-delay of 60 μs in TRFM mode (**b**). Right: The line profile illustrates quantitatively the difference in fluorescence intensity observed between conventional epifluorescence mode and TRFM mode. Images were acquired with loop-count of 250 and a 10-ms exposure period with 2 × 2 pixel binning and image intensifier gain of 60.

concentration of 650 μM (0.101) whereas at a similar concentration of BHHCT, the optical density was more than four-fold higher (0.429). The plots have a characteristic hump that results from the increasing concentration of 1,4 dioxane in the aqueous solution that tends to improve the solubility of the chelate.

DISCUSSION

The parent compound (BHHCT) from which BHHST is prepared is strongly activated and reacts with many common nucleophiles (hydroxyl and amino groups). This raised difficulties during attempts to purify BHHCT. However, we found that precipitation from hexane resulted in a product of greatly improved purity that gave excellent NMR signatures and a single spot when analyzed using reverse phase TLC plates (results not shown). Preparation of the propyl hydroxyl sulfonamide (step 4 in Fig. 1) proceeds rapidly with minimal side products when conducted in acetonitrile containing the nucleophilic catalyst dimethylaminopyridine (DMAP). The use of DMAP is indispensable for successful completion of step 5 in Figure 1, the activation of the hydroxyl group by di-(*N*-succinimidyl) carbonate, which in any case did not go to completion after refluxing for 2 days. The yield of 63%, however, is satisfactory and sufficient BHHST can be recovered from a gram of starting material for hundreds of conjugations. The β-diketone group of all the terphenyl derivatives tested was found to be labile and intolerant of passage through silica-gel chromatography columns. A satisfactory alternative method of obtaining milligram quantities of BBHST (in the form of a fine white precipitate) is based on precipitation from hexane. The hexane-precipitated BHHST gave a single spot on TLC plates and the NMR signature was clean, although the proton signal for the succinimide protons was deficient (50% of expected integral strength) for unknown reasons. The improved solution properties of BHHST were apparent when a DMF solution (containing BHHST) was added to the aqueous protein solution without some precipitate forming as was usually the case when BHHCT was employed for conjugations.

F/P Ratio and Yield of Immunoconjugate

Protein concentration of the monoclonal antibody (CRY104) was nearly twice (1.8×) that of the polyvalent goat antibody. However, both immunoconjugates were prepared using the same molar concentration of BHHST. Thus, for the anti-mouse preparation, the concentration of BHHST in relation to protein content was greater than that used for CRY104 and a higher F/P ratio resulted. Immunoglobulins vary considerably in their response to conjugation with activated compounds and affinity of the resultant immunoconjugate is dependent on the number and nature of the attached molecules. Protein yield is also impacted by similar factors that affect antibody affinity as well as the nature of the activating group used in the conjugation. Activation with reactive groups such as chlorosulfonic or cyanuric acid were reported to increase the risk of producing heavily labeled immunoconjugates with low affinity and increased risk of denaturation (Karsilayan

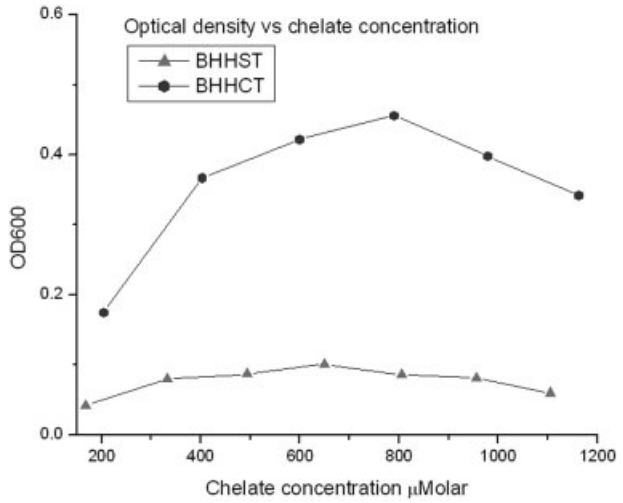

Fig. 7. Formation of micron-sized fragments of precipitated chelate occurred when a 1,4 dioxane solution of the chelates (26 mM) was added to a 0.1 M solution of $NaHCO_3$. A marked difference in the optical density was noted when comparing the results from BHHST and BHHCT additions with the latter compound observed to have more than 4-fold greater OD600 reading at a concentration of 650 μM. The higher optical density was presumed to be indicative of the increased hydrophobic nature of BHHCT.

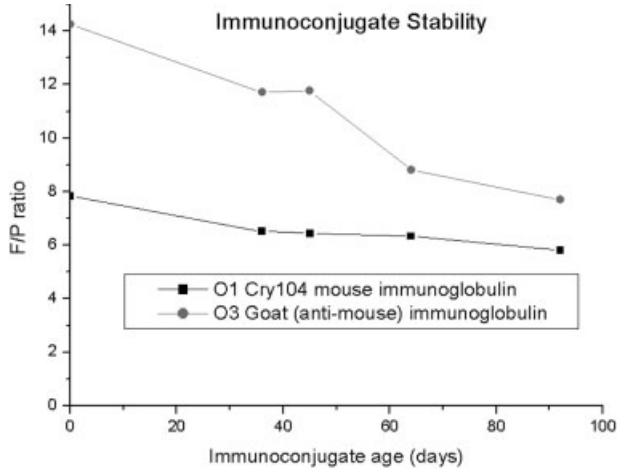

Fig. 8. Immunoconjugates with BHHST were prepared with monoclonal (Cry104) and polyvalent (Goat anti-mouse) immunoglobulin. Both preparations were observed to initially show a rapid drop in F/P over the first month before stabilizing to a slower rate of decay. Neither sodium azide or BSA stabilizing agents were present in the PBS buffer used to store the antibodies.

et al., 1997). Furthermore, protein loss can occur through protein aggregation and this process was reported to be sensitive to the pH of the conjugation buffer. It is interesting to note that in this work, the goat (anti-mouse) immunoglobulin was obtained with a higher F/P ratio, although at reduced yields (protein content) when compared to the mouse immunoglobulin (CRY104). When the goat immunoglobulin was treated with higher concentrations of BHHST, much lower yields were obtained (data not shown) presumably due to precipitation of the more heavily labeled fractions. Immunoconjugates with isothiocyanatobenzyl DTTA chelates at F/P ratios of 15 to 25 were reported to show little adverse effect on avidity when employed as reagents in the dissociation enhanced lanthanide fluoroimmunoassay (DELFIA) protocol.

When diazo couplings were employed, however, a maximum F/P ratio of 5 could be obtained before aggregation became a problem (Mukkala et al., 1989). Related studies have reported the optimal F/P ratio to be 1–5 (Dechaud et al., 1986). Higher F/P ratios (5–10) were reported to cause a 20–40% increase in aggregation of the labeled antibodies and a 10–50% decrease in immunoreactivity (Hnatowich et al., 1983; Paik et al., 1983).

Stability of the immunoconjugates was monitored by observing the F/P ratio spectro-photometrically and noting the point at which the F/P ratio decayed to half of that initially recorded (see Fig. 8). This method is far less problematic than attempting to measure fluorescence intensity of the immunoconjugate over time since fluorescence yield is strongly affected by buffer composition, pH, and the molar ratio of the europium ion to chelate concentration. Moreover, two spectral parameters must be measured to determine the F/P ratio since protein content and fluorophore concentration both need to be determined and this ensures some degree of internal calibration is maintained over the relatively long period (6 months) of monitoring. For immunoconjugate O_1, the half-life point was reached after 186 days and 81 days for the more heavily labeled goat immunoglobulin O_3. Protein content remained relatively constant over the observation period. The conjugation process was presumed to result in immunoconjugates with F/P ratios spanning a wide range and those at the upper limit of that range were at greater risk of denaturation. Thus, over a period of time, the heavily labeled immunoconjugate precipitated from solution resulting in a lower average F/P ratio, but protein concentration was relatively unaffected by the loss of this minor component. Immunoconjugates prepared with BHHCT were far less stable and most preparations completely precipitated after a day or two although some lasted a week. Half-life plots of BHHCT immunoconjugates are not shown since they offer little information due to the rapid and highly variable nature of their expiration.

Activity of BHHST is greater than that reported for iodoacetomido derivatives but at a lower scale than molecules activated by a dichlorotriazinyl moiety whereas isothiocyanate and succinimide activating groups have comparable activity. In a recent study with rabbit IgG immunoglobulin utilizing a 16-hour incubation period for the conjugation, F/P ratios of 1.2, 6.5, and 12 were reported for compounds activated with iodoacetomido, isothiocyanate, and dichlorotriazinyl groups, respectively (Takalo et al., 1994).

Removal of unbound BHHST from immunoconjugate on Sephadex G50 columns resulted in reduced yields when compared to the use of 50-Kda centrifugal filters. Furthermore, the F/P ratio of immunoconjugate purified on Sephadex columns was approximately half that obtained using the centrifugal filters (unpublished observations). The convenience of dealing with a small quantity of concentrated immunoconjugate was another factor that favored the use of centrifugal filters.

Reduction of non-specific fluorescence is of no benefit if the probe signal is similarly reduced and thus the

overall improvement in SNR is a critical parameter in evaluating the utility of TRFM. Intensity of the autofluorescent emission from the desmids was significant in conventional epifluorescence mode. Autofluorescence from the desmid spines was predominantly blue whereas the centre of the organism fluoresced pink; thus, spectral selection techniques would be useful for suppressing only a portion of the autofluorescent emission. Narrow pass-band filters are useful in suppressing a broad range of autofluorescence emission particularly where the probe fluorescence occupies a narrow pass-band, as in the case of lanthanide chelates (λ_{em} 617 nm; 10 nm FWHM). It is important to note that autofluorescence from the centre of the desmids falls within the pass band of the lanthanide chelate and would not be excluded by spectral filters. The efficiency of time-resolved fluorescence techniques to enhance SNR is independent of the autofluorescence emission wavelength and in this study yielded an 8.8-fold improvement in SNR for BHHST immunolabeled *Cryptosporidium* oocysts and a 11.1-fold improvement in SNR for labeled *Giardia* cysts. Although images were captured with a grey scale resolution of 4,096 levels (12-bit digital range), conversion to 256-levels (8-bit range) was performed for the reasons discussed in the Introduction. Pixel brightness was adjusted by varying the loop-count (the number of capture cycles per image) to avoid saturation of pixel amplitude (pixel values of 256). Manipulation of brightness to prevent pixel saturation also has the effect of reducing the SNR (see Eq. 3) and hence the images included in this report were optimized for visual clarity rather than for the best SNR. Furthermore, as a consequence of the 8-bit scale employed for our TRFM, the best SNR that could possibly be achieved is 255:1. The human eye, however, can distinguish only approximately 60 grey scales and the background of the images captured in TRFM mode (see Figs. 4b and 6b) appears uniformly black, even though the average pixel value for these ranges lies between 13 to 17 (8-bit range). SNR enhancement is controlled to a large extent by the gain setting on the image intensifier. However, at high gains (>60%) the images acquire a grainy "night-vision" effect that significantly degrades image quality. At the different gain settings used for this work, contrast was unaffected since all pixel brightness values (intensity) were linearly varied and, thus, the use of a ratio of ratios as defined by Eq. 3 may be reliably used to estimate ΔSNR. The degree to which autofluorescence was suppressed by our TRFM (~11:1) is significantly less than the 1:5,500 figure reported for an argon-ion laser excited TRFM fitted with a gated microchannel plate image intensifier (Hennink et al., 1996). This level of suppression was reported for a model system employing fluorescent beads rather than environmental samples. The microscope was used to identify phosphorescent emission from Pt-porphine impregnated Sephadex beads against fluorescein polymer microspheres. The platinum and palladium chelates used for this work, however, were reported to be very sensitive to oxygen that acts to markedly reduce fluorescence quantum yield and lifetime (de Haas et al., 1999).

Probe fluorescence intensity has a large effect on the observed SNR and previous studies that employed alternative chelates for time-resolved fluorescence studies were reported to be hampered by low fluorescence yield of the probe (Diamandis et al., 1989; Marriott et al., 1994). Marriot et al. (1994) increased fluorescence yield of the label by employing a primary immunolabel conjugated with biotin. This primary label was then made fluorescent by reaction with streptavidin cross-linked to thyroglobulin multiply labeled with fluorescent europium-chelate. Other techniques that have been used to increase probe signal strength include tyramide signal amplification (TSA) protocol to deposit biotin at immunolabeled sites for subsequent binding to a fluorescent streptavidin-chelate conjugate (de Haas et al., 1996). The fluorescence intensity obtained with the BHHST immunoconjugate reported here was sufficient to avoid the need for complex and time-consuming fluorescence enhancement strategies. Furthermore, unlike other lanthanide chelates that are reported to require special embedding medium (Merckoglass) in which conventional fluorophores emit weakly (de Haas et al., 1996), the BHHST immunoconjugates are strongly fluorescent in bicarbonate buffer containing a trace of TOPO. No evidence of non-specific labeling was observed in the slide preparations. However, the PVA-FEB buffer did cause some increase in background (see Fig. 6) since this matrix can excite low-level fluorescence from europium ions. Incomplete washing of the filter was also suspected to have resulted in the carryover of a trace of immunoconjugate since the background was a little higher than normal.

CONCLUSION

The primary aim of this work was to develop a technique that facilitates the discrimination of probe fluorescence from spurious background autofluorescence. TRFM has proven to be a successful method that can satisfy the primary aim, provided suitable fluorescence probes are employed. The strongly fluorescent europium chelate BHHCT and its homologues have been successfully employed for time-resolved fluorescence studies (Connally et al., 2002; Sueda et al., 2000; Wu and Zhang, 2002; Yuan and Matsumoto, 1996). The hydrophobic nature of the parent compound, however, leads to unstable immunoconjugates that are difficult to prepare. The hydrophobic nature of BHHCT was reduced by appending a short water soluble tether to the molecule to form BHHST. The short tether also projects the hydrophobic portion of the molecule away from the binding point on the protein and this was anticipated to reduce (potentially disruptive) interaction between the bound fluorophore and the protein chain. Immunoconjugates prepared with BHHST were far more stable than those prepared with BHHCT and both *Cryptosporidium* and *Giardia* pathogens were labeled in situ with a BHHST immunoglobulin conjugate that was already 36 days old. It is worthwhile to note the relatively low F/P of the anti-*Cryptosporidium* conjugate (F/P of 6) that was still effective in labeling oocysts for TRFM analysis. Stability of the immunoconjugate is known to be inversely related to the F/P ratio and the activity of the antibody tends to decrease markedly as F/P ratio increases (Karsilayan et al., 1997). Sodium azide, dimethyl sulfoxide, bovine serum albumin, some sugars, and glycerol have all been reported to increase the stability of some immunoglobulin conjugates (Esteves et al., 2000; Savellano and Hasan, 2003). Stability of the BHHST immunoconjugates in phosphate buffered saline was determined

without the addition of any stabilizing agents and a further increase in storage lifetime could be reasonably anticipated if appropriate stabilizing reagents were employed.

As reported in the Discussion, some time-resolved fluorescence microscopes strongly suppressed autofluorescence but fluorescence intensity of the probe was poor and required enhancement. Image processing (thresholding) may be applied to completely eliminate background provided sufficient contrast exists between the target probe and non-specific autofluorescence. Thresholding is a technique that sets all pixels below a certain threshold value to zero and is well suited for processing the high-contrast images obtained from the TRFM described here. Threshold-processed images can then be analyzed by machine-vision systems to automate the analysis of samples that are difficult and tedious for human operators due to the high level of background autofluorescence.

The chemical modifications made to BHHCT to produce BHHST are general and could be applied with equal ease to the other homologues of BHHCT that have been reported to be useful fluorescent probes for time-resolved fluorescence studies. BTBCT is the trifluoromethyl homologue of BHHCT and was reported to be 8-fold brighter than the parent compound, but immunoconjugates prepared with BTBCT were observed to precipitate at concentrations as low as 50 $\mu g.ml^{-1}$ (Wu and Zhang, 2002). Modification of BTBCT to carry a succinimide tether could potentially deliver a probe with improved fluorescence yield that is soluble and stable in aqueous solutions. BHHCT and BTBCT have both been applied as probes in time-resolved fluorescence immunoassays. However, to our knowledge, we are the first to report detection of micro-organisms within strongly autofluorescent environments using TRFM.

REFERENCES

Baschong W, Suetterlin R, Laeng RH. 2001. Control of autofluorescence of archival formaldehyde-fixed, paraffin-embedded tissue in confocal laser scanning microscopy (CLSM). J Histochem Cytochem 49:1565–1572.

Clancy B, Cauller LJ. 1998. Reduction of background autofluorescence in brain sections following immersion in sodium borohydride. J Neurosci Methods 83:97–102.

Connally R, Veal D, Piper J. 2002. High resolution detection of fluorescently labeled microorganisms in environmental samples using time-resolved fluorescence microscopy. FEMS Microbiol Ecol 41: 239–245.

Connally R, Veal D, Piper J. 2004. Flashlamp excited time-resolved fluorescence microscope suppresses autofluorescence in water concentrates to deliver 11-fold increase in signal to noise ratio. J Biomed Optics 9:725–734.

de Haas RR, Verwoerd NP, Van Der Corput MP, Van Gijlswijk RP, Siitari H, Tanke HJ. 1996. The use of peroxidase-mediated deposition of biotin-tyramide in combination with time-resolved fluorescence imaging of europium chelate label in immunohistochemistry and in-situ hybridization. J Histochem Cytochem 44:1091–1099.

de Haas R, van Gijlswijk RPM, van der Tol EB, Veuskens J, van Gijssel HE, Tijdens RB, Bonnet J, Verwoerd NP, Tanke HJ. 1999. Phosphorescent platinum/palladium coproporphyrins for time-resolved luminescence microscopy. J Histochem Cytochem 47:183–196.

Dechaud H, Bador R, Claustrat F, Desuzinges C. 1986. Laser-excited immunofluorometric assay of prolactin, with use of antibodies coupled to lanthanide-labeled diethylenetriaminepentaacetic acid. Clin Chem 32:1323–1327.

Diamandis EP, Morton RC, Reichstein E, Khosravi MJ. 1989. Multiple fluorescence labeling with europium chelators. Application to time-resolved fluoroimmunoassays. Anal Chem 61:48–53.

Esteves MI, Quintilio W, Sato RA, Raw I, De Araujo PS, Da Costa MHB. 2000. Stabilization of immunoconjugates by trehalose. Biotechnol Lett 22:417–420.

Hennink RJ, de Haas R, Verwoerd NP, Tanke HJ. 1996. Evaluation of a time-resolved fluorescence microscope using a phosphorescent Pt-porphine model system. Cytometry 24:312–320.

Hnatowich DJ, Childs RL, Lanteigne D, Najafi A. 1983. The preparation of DTPA-coupled antibodies radiolabeled with metallic radionuclides: an improved method. J Immunol Methods 65:147–157.

Karsilayan H, Hemmila I, Takalo H, Toivonen A, Pettersson K. 1997. Influence of coupling method on the luminescence properties, coupling efficiency, and binding affinity of antibodies labeled with europium (III) chelates. Bioconjugate Chem 8:71–75.

Latva M, Mukkala VM, Matachescu C, Rodriguez-Ubis JC, Kankar J. 1997. Correlation between the lowest triplet state energy level of the ligand and lanthanide(III) luminescence quantum yield. J Luminesc 75:149–169.

Li M, Selvin PR. 1995. Luminescent polyaminocarboxylate chelates of terbium and europium: the effect of chelate structure. J Am Chem Soc 117:8132–8138.

Marriott G, Heidecker M, Diamandis EP, Yan-Marriott Y. 1994. Time-resolved delayed luminescence image microscopy using an europium ion chelate complex. Biophys J 67:957–965.

Mukkala VM, Mikola H, Hemmila I. 1989. The synthesis and use of activated N-benzyl derivatives of diethylenetriaminetetraacetic acids: alternative reagents for labeling of antibodies with metal ions. Anal Biochem 176:319–325.

Paik CH, Ebbert MA, Murphy PR, Lassman CR, Reba RC, Eckelman WC, Pak KY, Powe J, Steplewski Z, Koprowski H. 1983. Factors influencing DTPA conjugation with antibodies by cyclic DTPA anhydride. J Nucl Med 24:1158–1163.

Savellano MD, Hasan T. 2003. Targeting cells that overexpress the epidermal growth factor receptor with polyethylene glycolated BPD verteporfin photosensitizer immunoconjugates. Photochem Photobiol 77:431–439.

Sorensen AH, Torsvik VL, Torsvik T, Poulsen LK, Ahring BK. 1997. Whole-cell hybridization of Methanosarcina cells with two new oligonucleotide probes. Appl Environ Microbiol 63:3043–3050.

Staughton TJ, McGillicuddy CJ, Weinberg PD. 2001. Techniques for reducing the interfering effects of autofluorescence in fluorescence microscopy: improved detection of sulphorhodamine B-labelled albumin in arterial tissue. J Microsc 201:70–76.

Sueda S, Yuan J, Matsumoto K. 2000. Homogeneous DNA hybridization assay by using europium luminescence energy transfer. Bioconjugate Chem 11:827–831.

Tagliaferro P, Tandler CJ, Ramos AJ, Pecci Saavedra J, Brusco A. 1997. Immunofluorescence and glutaraldehyde fixation. A new procedure based on the Schiff-quenching method. J Neurosci Methods 77:191–197.

Takalo H, Mukkala V-M, Mikola H, Liitti P, Hemmila I. 1994. Synthesis of europium(III) chelates suitable for labeling of bioactive molecules. Bioconjug Chem 5:278–282.

Vereb G, Jares-Erijman E, Selvin PR, Jovin MT. 1998. Temporally and spectrally resolved imaging microscopy of lanthanide chelates. Biophys J 74:2210–2222.

Vesey G, Slade JS, Byrne M, Shepherd K, Fricker CR. 1993. A new method for the concentration of *Cryptosporidium* oocysts from water. J Appl Bacteriol 75:82–86.

Wu F-B, Zhang C. 2002. A new europium β-diketone chelate for ultrasensitive time-resolved fluorescence immunoassays. Anal Biochem 311:57–67.

Yuan J, Matsumoto K. 1996. Synthesis of a new tetradentate β-diketonate-europium chelate that can be covalently bound to proteins in time-resolved fluorometry. Anal Sci 12:695–699.

Yuan J, Matsumoto K. 1998. A new tetradentate β-diketonate-europium chelate that can be covalently bound to proteins for time-resolved fluoroimmunoassay. Anal Chem 70:596–601.

Yuan J, Wang G, Majima K, Matsumoto K. 2001. Synthesis of a terbium fluorescent chelate and its application to time-resolved fluoroimmunoassay. Anal Chem 73:1869–1876.